Accepted Manuscript

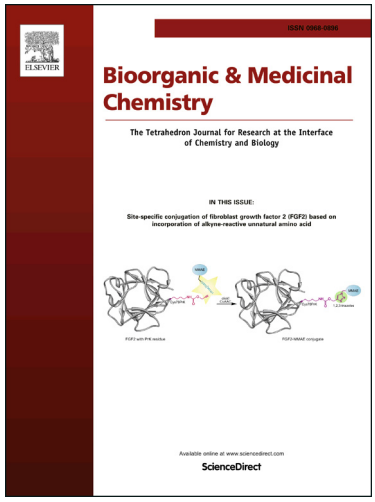

Design, synthesis and biological evaluation of 2-phenylquinoline-4-carboxamide derivatives as a new class of tubulin polymerization inhibitors

Li Zhu, Kaixiu Luo, Ke Li, Yi Jin, Jun Lin

PII: S0968-0896(17)31519-5
DOI: http://dx.doi.org/10.1016/j.bmc.2017.09.004
Reference: BMC 13964

To appear in: *Bioorganic & Medicinal Chemistry*

Received Date: 26 July 2017
Revised Date: 5 September 2017
Accepted Date: 6 September 2017

Please cite this article as: Zhu, L., Luo, K., Li, K., Jin, Y., Lin, J., Design, synthesis and biological evaluation of 2-phenylquinoline-4-carboxamide derivatives as a new class of tubulin polymerization inhibitors, *Bioorganic & Medicinal Chemistry* (2017), doi: http://dx.doi.org/10.1016/j.bmc.2017.09.004

Journal Name

ARTICLE

Design, synthesis and biological evaluation of 2-phenylquinoline-4-carboxamide derivatives as a new class of tubulin polymerization inhibitors

Received 00th January 20xx,
Accepted 00th January 20xx

DOI: 10.1039/x0xx00000x

www.rsc.org/

Li Zhu [a‡], Kaixiu Luo [a‡], Ke Li [b‡], Yi Jin*[a] and Jun Lin*[a]

A novel series of 2-phenylquinoline-4-carboxamide derivatives was synthesized, characterized and evaluated for its antiproliferative activity against five cancer cell lines, Hela, SK-OV-3, HCT116, A549 and MDA-MB-468, and a normal human fetal lung fibroblastic cell line, MRC-5. Among them, compound **7b** displayed potent cytotoxic activity in vitro against SK-OV-3 and HCT116 cell lines with IC_{50} values of 0.5 and 0.2 μM, respectively. In general, the antiproliferative activity was correlated with the binding property of the colchicine binding site and inhibitory effect on tubulin polymerization. In addition, immunofluorescence and flow cytometry analysis revealed that selected compounds caused disruption of the mitotic spindle assembly and G_2/M phase arrest of the cell cycle, which correlated with proliferation inhibitory activity. Molecular docking analysis demonstrated the interaction of **7b** at the colchicine binding site of tubulin. These results indicate these compounds are promising inhibitors of tubulin polymerization for the potent treatment of cancer.

Introduction

Microtubules are key components of the cytoskeleton which are protein polymers formed by dynamic polymerization and depolymerization of α- and β-tubulin heterodimers, and are involved in various important biological functions, including cell structure maintenance, cell division, signal transduction and intracellular transport.[1-4] In the mitotic phase of the cell cycle, microtubules are highly dynamic, and rapidly arrange and rearrange depending on the cell's needs.[5] Disruption of the dynamic equilibrium can induce cell cycle arrest in G_2/M phase, resulting in cell death.[6-8] Given their essential role in cellular processes, microtubules have become attractive chemotherapeutic targets for the design and synthesis of new antimitotic anticancer agents.[2, 9] A large number of natural products and their analogues have been identified to act on microtubule inhibitors, and some of them have been used clinically in the treatment of different cancers over the past decade.[2] These agents can be separated into three groups: the taxane site for microtubule stabilizers, the vinca site and the colchicine site for microtubule destabilizers.[10] Taxoids and vincristine alkaloids have been widely used as first-line antitumour drugs in clinical treatments. However, the emergence of drug resistance, high toxicity and complex synthesis greatly limit their therapeutic applications. Colchicine is the first colchicine site inhibitor, which played an important role in deciphering the properties and functions of tubulin and microtubules. Even though colchicine is not used clinically because of its high toxicity,[11] other diverse small molecules that also bind at the colchicine site on tubulin have been discovered recently and have come under intensive investigation. The most representative compounds include natural products and their derivatives, as well as synthetic small molecules, as shown in **Fig. 1**. Because of their therapeutic potential, synthetic accessibility and structural diversity, small molecular colchicine site binders such as **CA-4**[12] and **ZD6126**[13] have been tested clinically, whereas **ABT-751**, **BNC105** and **ELR510444** showed promising anticancer effects.[14-16]

2-Phenylquinoline-4-carboxamide derivatives have been found to exhibit a variety of biological activities such as antitumor, anti-inflammatory, antibacterial, antiviral, antituberculosis and immunosuppression activity.[17-19] For example, **STX-0119** (**Fig. 2a**), a novel small-molecule STAT3 dimerization inhibitor, displays good efficacy against human lymphoma cells by down-regulating STAT3 target genes and leading to apoptosis in tumours.[20] **HJC0123**, a novel orally bioavailable STAT3 inhibitor, has demonstrated potent anticancer effects against a negative breast cancer MDA-MB-231 xenograft tumour in vivo by down-regulation of phospho-STAT3 and induction of apoptosis in breast and pancreatic cancer cells.[17] To date, no studies have reported that 2-phenylquinoline-4-carboxamide derivatives are active as tubulin polymerization inhibitors. Recently, we performed a structure-based virtual screening against the colchicine binding pocket from a screening library containing approximately

[a] Key Laboratory of Medicinal Chemistry for Natural Resource (Yunnan University), Ministry Education, School of Chemical Science and Technology, Yunnan University, Kunming, 650091, P. R. China.
[b] Department of Medical Oncology, the Third Affiliated Hospital of Kunming Medical University, Yunnan Tumor Hospital, Kunming 650031, P. R. China.
‡ the authors contributed equally to this work.
* Corresponding author. Tel./fax: +86-871-65031633 (J. L.).
E-mail: jinyi@ynu.edu.cn (Y. Jin); linjun@ynu.edu.cn (J. Lin).
Electronic Supplementary Information (ESI) available: [details of any supplementary information available should be included here]. See DOI: 10.1039/x0xx00000x

100,000 diverse drug-like compounds. The results showed that more than ten compounds are 2-phenylquinoline-4-carboxamide derivatives in the top 100 highest scoring candidates. From 2007 to 2015, Metwally et al reported that a series of pyrimido[4,5-c]quinolin-1(2H)-one derivatives which have similar structures to 2-phenylquinoline-4-carboxamide had weak to medium antimitotic activity.[21-24]

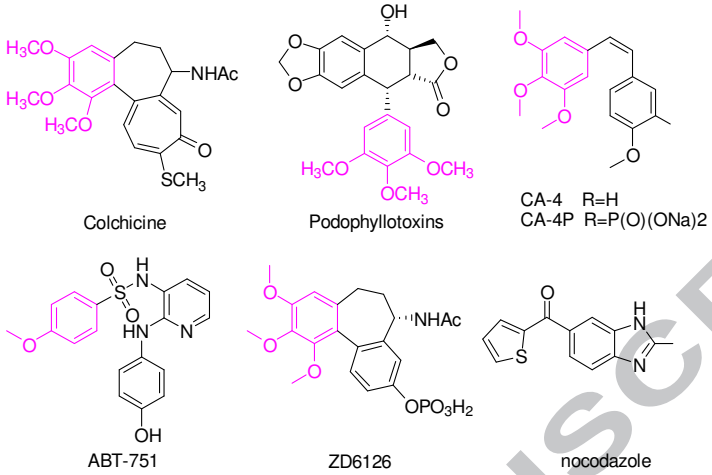

Fig. 1 Representative tubulin inhibitors act through colchicine site.

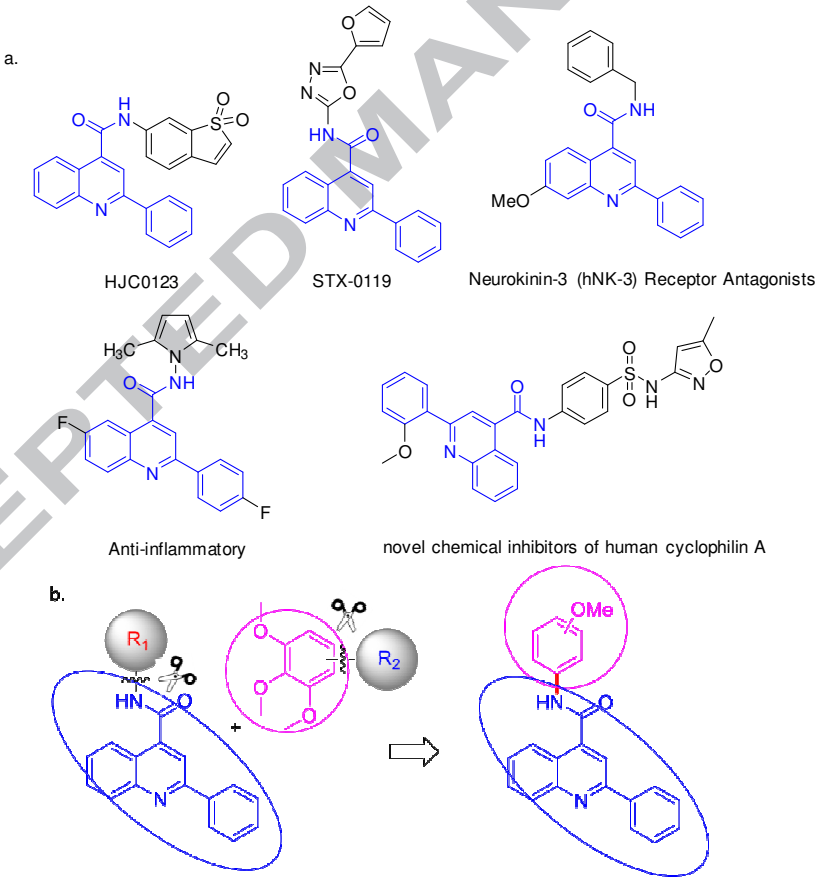

Fig. 2 a).Derivative of 2-phenyl-4-quinolinecarboxylic acid with biological activity. b). Design strategy of 2-phenylquinoline-4-carboxamide derivatives.

Journal Name

ARTICLE

Therefore, 2-phenylquinoline-4-carboxamide represents a potential lead compound to explore novel tubulin polymerization inhibitors as new cancer agents. Meanwhile, the trimethoxyphenyl are essential pharmacophore contributing to the binding of colchicine.[25] Specifically, the hydroxyl and methoxy groups on the phenyl ring of CA-4 are known to exhibit interactions with the colchicine binding site.[26] On the basis of scaffold hopping of privileged scaffolds from known bioactive compounds, our modification strategy of 2-phenylquinoline-4-carboxamide was focused on hybridizing two pharmacophoric units to design improved anticancer agents to lead the development of a variety of potent, small-molecule tubulin binder (**Fig. 2b**).

Herein, we would like to describe our efforts on the biological evaluation and structural optimization of the new 2-phenylquinoline-4-carboxamide-based tubulin inhibitors. The synthesized compounds were evaluated for their biological activity toward one normal human cell line and five different human tumour cell lines. Among these derivatives, compound **7b** exhibited the most potent antiproliferative activity against Hela, SK-OV-3, HCT116, A549 and MDA-MB-468 cells (IC_{50} = 1.6, 0.5, 0.2, 5.7 and 10.8 μM, respectively). The binding interactions between tubulin and compound **7b** were also investigated by using computer-based docking studies.

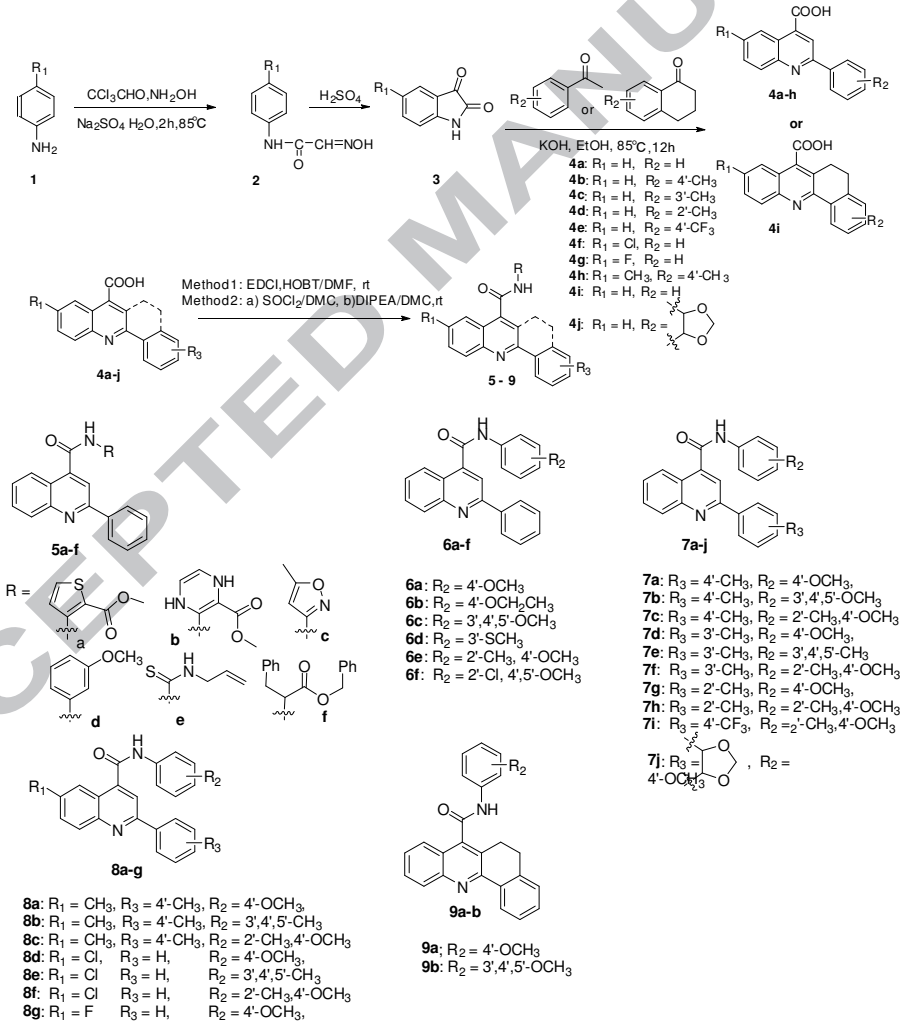

Scheme 1 Synthesis of 2-phenyl-4-quinolinecarboxylic acid.

Journal Name

ARTICLE

Results and discussion

Chemistry

The general synthetic approach for 2-phenyl-4-quinoline carboxylic acid (**4**) is illustrated in **Scheme 1**. Firstly, substituted anilines reacted with hydroxylamine hydrochloride and chloral hydrate to form isonitrosoacetanilide **2**, followed by a Sandmeyer reaction with concentrated sulfuric acid to get desired product **3**. Then the 2-phenylquinoline-4-carboxylic acid compounds (**4a–n, Table 1**) were obtained in high yields through the Pfitzinger reaction.[27]

For the synthesis of compounds **5–9**, two methods were performed according to the reaction activity of the start materials. In the first one, 4-carboxamide products were obtained using compounds **4** and different anilines as raw materials in the presence of a condensing agent (CDI+DCC) and NMM and DMF as solvents at room temperature. The reaction yields were from 70% to 90%. In the second method, compounds **4** were firstly converted to the corresponding acyl chloride via reaction with a small excess of $SOCl_2$ in THF. Then, the desired products **5–9** were successfully obtained via the reaction of the above-mentioned acyl chlorides with different anilines in the presence of triethylamine (Et_3N) and THF as solvent at room temperature. We optimized these two methods by screening the reaction conditions (see supplementary information).

Table 1 Cytotoxic activity (IC_{50} in μM) of compounds **5–9** against different cancer cell lines

Entry	Compound	Hela	SK-OV-3	HCT116	A549	MDA-MB-468	MRC-5
1	**5a**	34.5	20.3	22.6	48.7	36.8	46.3
2	**5b**	36.8	38.9	29.5	> 50	> 50	> 50
3	**5c**	> 50	36.6	25.8	37.9	46.2	> 50
4	**5d**	40.5	17.4	12.9	32.5	34.7	43.8
5	**5e**	> 50	> 50	> 50	> 50	> 50	> 50
6	**5f**	> 50	> 50	36.1	> 50	> 50	> 50
7	**6a**	32.5	12.8	4.9	20.5	34.7	40.5
8	**6b**	> 50	45.8	49.1	> 50	> 50	> 50
9	**6c**	12.7	5.4	2.7	17.9	18.9	38.8
10	**6d**	45.8	36.8	48.3	> 50	42.8	> 50
11	**6e**	16.4	8.4	7.8	23.7	20.1	> 50
12	**6f**	42.6	36.3	> 50	> 50	42.8	> 50
13	**7a**	25.2	6.3	3.7	18.5	35.2	47.8
14	**7b**	1.6	0.5	0.2	5.7	10.8	31.9
15	**7c**	9.5	4.2	1.7	11.6	17.4	48.1
16	**7d**	30.2	12.4	9.4	30.5	> 50	> 50
17	**7e**	5.3	10.6	11.6	17.8	32.7	42.3
18	**7f**	10.4	15.3	14.6	23.6	32.1	> 50
19	**7g**	42.8	36.7	31.4	> 50	> 50	> 50
20	**7h**	> 50	42.2	43.6	45.7	41.6	> 50
21	**7i**	> 50	> 50	47.3	> 50	> 50	> 50

22	**7j**	> 50	43.4	> 50	46.3	> 50	> 50
23	**8a**	16.4	8.3	10.4	29.7	32.4	> 50
24	**8b**	13.5	6.2	5.2	20.3	37.1	42.7
25	**8c**	20.4	12.3	11.9	30.1	46.1	> 50
26	**8d**	40.2	20.3	24.8	> 50	> 50	> 50
27	**8e**	> 50	24.1	36.4	> 50	> 50	> 50
28	**8f**	> 50	34.2	27.4	> 50	> 50	> 50
29	**8g**	> 50	29.7	34.2	> 50	> 50	> 50
30	**9a**	> 50	37.6	39.5	> 50	> 50	> 50
31	**9b**	> 50	32.5	> 50	> 50	> 50	> 50
32	**Colchicine**	0.5	0.05	0.01	0.02	0.06	0.09
33	**CA-4**	0.3	0.01	0.06	0.09	0.2	9.5

Biological results and discussion

In vitro antiproliferative activity

All the newly synthesized 2-phenylquinoline-4-carboxamide derivatives were evaluated for their antiproliferative activities against five human cancer cell lines: Hela (human cervical cancer), SK-OV-3 (human ovarian cancer), HCT116 (human colon cancer), A549 (human lung cancer), MDA-MB-468 (human breast cancer) and one normal human cell line (MRC-5) by means of sulforhodamine B colorimetric assay. The results are summarized as IC_{50} values in **Table 1**. Two well-known tubulin inhibitors, CA-4 and colchicine, were used as positive compounds to validate the screening conditions. It was found that colchicine potently inhibited the growth of Hela, SK-OV-3, HCT116, A549 and MDA-MB-468 cancer cells with IC_{50} values of 0.5, 0.05, 0.01, 0.02 and 0.06 μM, respectively, which is highly comparable to the reported data.[28-31] CA-4 also displayed similar antiproliferative activity. We firstly screened six different 4-carboxamide derivatives substituted with heterocycles (thiophene **5a**, isoxazole **5b** and dihydropyrazine **5c**), benzene **5d**, N-allylethanethioamide **5e**, or phenyl- propanoate **5f**). The heterocycles and benzene-substituted compounds (**5a–d**) showed low to moderate cytotoxic activity with IC_{50} values against Hela, SK-OV-3, HCT116, A549 and MDA-MB-468 cancer cell lines. However, aliphatic-substituted compounds (**5e–f**) were inactive against these five cancer cell lines. The most active compound **5d** exhibited better antiproliferative activity against SK-OV-3 and HCT116 cell lines, with the IC_{50} values of 17.4 and 12.9 μM indicating that benzene-substituted 4-carboxamide derivatives are a good starting point for further structural optimization.

Then we studied the potential impact of the 3'-methoxyphenyl moiety in **5d** on its cytotoxic activity by replacing it with 4'-methoxyphenyl (**6a**), 4'-ethoxyphenyl (**6b**), 3',4',5'-trimethoxyphenyl (**6c**), 3'-methylthiophenyl (**6d**), 2'-methyl-4'-methoxyphenyl (**6e**) and 2'-chloro-4',5'-dimethoxyphenyl (**6f**) groups. It was found that the position and quantity of methoxy and methyl moieties obviously affect its biological activity. When the 3'-methoxy group was displaced by 3',4',5'-trimethoxy (**6c**) or 2'-methyl-3'-methoxy moieties (**6e**), the antiproliferative activity was obviously improved to display IC_{50} values of 5.4 and 8.4 μM against the SK-OV-3 cell line and 2.7 and 7.8 μM against the HCT116 cell line, respectively. 4'-Methoxyphenyl (**6a**) showed similar biological activity to 3'-methoxyphenyl (**5d**). However, 4'-ethoxyphenyl (**6b**) lost its inhibition potency against five cancer cell lines, which means that no large substituted groups are suitable at this position. Meanwhile, when a methoxy group was changed to a methylthio moiety, or a chlorine atom was introduced into the phenyl ring, the antiproliferation potency of cancer cell lines was dramatically decreased.

We further investigated the effects of R_3 substitution on cytotoxic activity by fixing R_2 as 4'-methoxy, 3',4',5'-trimethoxy or 2'-methyl-4'-methoxy, respectively. It was found that R_3 also exhibited a great impact on the antiproliferative activity of the resulting compounds. When the 4'-hydrogen atom in **6c** was replaced with a p-methyl group (**7b**), the potency was dramatically increased (about tenfold) with IC_{50} values of 0.5 and 0.2 μM against SK-OV-3 and HCT116, respectively. Further investigation suggested that the meta- or ortho-methyl substitution in **7d–h** decreased the potency of the antiproliferative activity against all five cancer cell lines. When the electron-withdrawing moiety 4'-CF_3 or a 1,3-dioxolane ring was introduced into R_3, compounds **7i** and **7j** lost their cytotoxic activity.

The effects of R_1 substitution on the antiproliferation of cancer cell lines were also investigated by fixing R_2 as 4'-methoxy, 3',4',5'-trimethoxy or 2'-methyl-4'-methoxy and R_3 as 4'-methyl or H. When the R_1 group was fixed as a methyl moiety, it was found that **8a**, **8b** and **8c** maintained moderately potent antiproliferative activity against Hela, SK-OV-3, HCT116 and A549 cell lines. However, when R_1 was replaced by an electron-withdrawing Cl or F atom, compounds **8d–g** lost the cytotoxic activity against all five cancer cell lines.

Finally, we investigated the quinoline-[2,3]-fused cyclic compounds **9a** and **9b**. It was found that the fused cyclic structures resulted in the loss of antiproliferative activity potency, even if the R_2 substitution was fixed as a 4'-methoxy or 3',4',5'-trimethoxy moiety.

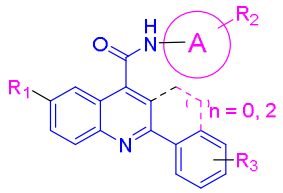

Cytotoxicity order
(n = 0) > (n = 2)
(A = aromatic) > (A = aliphatic)
R_1 = H > CH_3 > F, Cl
R_2 = 3',4',5'-OCH_3 > 4'-OCH_3 > 2'-CH_3, 4'-OCH_3 > 3'-SCH_3
R_3 = 4'-CH_3 > 3'-CH_3 or 2'-CH_3 > 4'-CF_3

Fig. 3 SAR of the 2-phenylquinoline-4-carboxamide derivatives

The SAR studies were concluded for these 2-phenylquinoline-4-carboxamide derivatives (**Fig. 3**). In particular, the quinoline-[2,3]-fused cyclic compounds or aliphatic substituted in section A dramatically decreased the potency of antiproliferative activity. Specifically, methoxy group substituted at R_2 are benefit for cytotoxic activity, while the substitution at R_1 group will decrease the biological activity, especially the electro-withdraw group, e.g. CF_3, resulted in the loss of antiproliferative activity potency.

It is worth noting that all active compounds, such as **6c** and **7b**, exhibited poor cytotoxic activity against the human normal cell line MRC-5, but the positive compounds colchicine and CA-4 showed dramatic antiproliferative activity against this cell line.

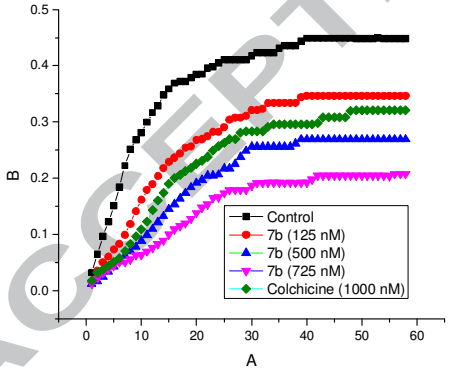

Fig. 4 Effects of **7b** on in vitro tubulin polymerization assay. Colchicine (1 μM) was used as a reference, while ethanol (1% v/v) was used as a vehicle control. The reaction was started by warming the solution from 4 to 37 °C. Purified bovine tubulin and GTP were mixed in a 96-well plate. The effect on tubulin assembly was monitored in a Spectramax 340PC spectrophotometer at 340 nm at 60 s intervals for 60 min at 37 °C.

Tubulin polymerization assay

To examine whether the cytotoxic activity of compound **7b** was related to the interaction with tubulin, it was subjected to evaluation by tubulin assembly assay in a cell-free in vitro assay. To test this, different concentrations of compound **7b** were incubated with tubulin protein, using colchicine as a positive control. The results were obtained by spectrophotometric measurement at λ = 340 nm. As shown in **Fig. 4**, compound **7b** proved to be a strong inhibitor of tubulin polymerization in different concentration (125, 500, 750 nM, respectively), showing a trend similar to colchicine. The results demonstrated that inhibition of tubulin polymerization of compound **7b** is correlated with growth inhibition.

Competitive colchicine binding assay

Compound **7b** was revealed as the parallel inhibitor similar to that of CA-4 in the polymerization of tubulin. Thus we explored whether this compound could bind to the colchicine site of tubulin by using a fluorescence-based assy.[32] we found an increase in the fluorescence of the tubulin-colchicine complex in the presence of **7b**, CA-4. This effect was similar to the fact that CA-4 generates increased fluorescence upon binding at the colchicine site (**Fig. 5a**).[33] The result of experiments were showed that tested compound **7b** has significant affinity toward the colchicine binding site at low concentrations, whereas at higher concentrations **7b** exhibited a steady increase in its binding affinity. Vinblastine was used as a negative control, which is known to bind at a different site, and it did not show any effect on the tubulin-colchicine complex. Therefore, this experiment suggests that compound **7b** bind at the colchicine site on tubulin.

Effect on cellular cyclin-B1 by immunoblot analysis

Cyclin-B1 is induced at the G2/M boundary to promote cell division. This protein is one of the important regulatory proteins of mitosis and accumulation of cyclin-B1 is an indication for G2/M arrest. Since compound 7b arrests the cell at G2/M phase, we investigated its effect on cyclin-B1 protein. Thus, we treated the HCT116 cells with the compound 7b at different concentrations (0.06 - 1.0 μM) for 24h and performed the immunoblot analysis for cyclin-B1 and tubulin as loading control. Therefore, the accumulation of cyclin-B1 levels suggests that these conjugates demonstrate cytotoxic effect through cell cycle arrest at mitosis. This data suggests that treatment by 7b induces a mitotic arrest, with the activation of spindle checkpoint in 24h as shown in **Fig. 5b.**

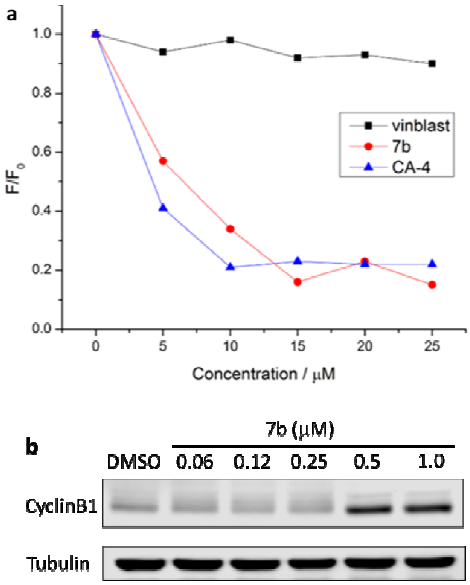

Fig. 5 a). Fluorescence-based colchicine competitive binding assays of compound **7b**. CA-4 was used as positive control, and vinblastine was used as a negative control; **b)**. Western blot analysis of Cyclin-B1: Treatment of HCT116 cells with 0.06, 0.12, 0.25, 0.5 and 1.0 μM concentrations of **7b** for 24 h resulted an increase in cyclinB1 levels significantly. Tubulin was employed as loading control and DMSO as negative control.

Immunofluorescence staining

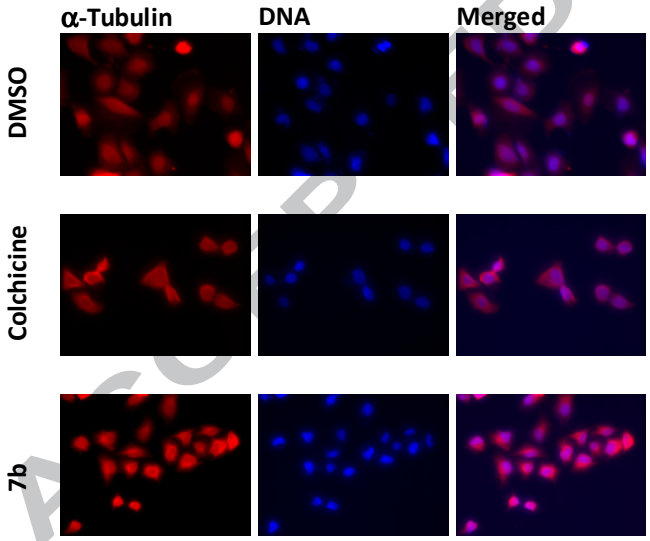

Fig. 6 Effect of **7b** on the organization of the cellular microtubule network. HCT116 cells treated with **7b** and colchicine were fixed and stained with α-tubulin, and then counterstained with 4, 6-diamidino-2-phenylindole (DAPI). Microtubules and unassembled tubulin are shown in red. DNA, stained with DAPI, is shown in blue.

Microtubule depolymerizing agents disrupt the dynamic equilibrium of tubulin and prevent the formation of spindles, subsequently inducing cell cycle arrest in G_2/M phase. In order to examine the tubulin inhibition of 2-phenylquinoline-4-carboxamide derivatives in cultured HCT116 cells, the immunofluorescence technique was used to determine the effects of **7b** on microtubule skeletons by confocal microscopy. In this study, DMSO was used as a blank control and colchicine was used as a positive control. As shown in **Fig. 6**, we observed a well-organized microtubule structure in control cells. In contrast, cells treated with colchicine and **7b** showed disrupted microtubule organization at 0.5 μM. These results support the potential inhibitory function of **7b** against tubulin.

Cell cycle analysis

Anticancer drugs are known to interact with cells, leading to cell growth arrest or cell death. To gain further insight into the mode of action, the effects of compound **7b** on HCT116 cell cycle progression was studied by flow cytometry against HCT116 human cancer cells. HCT116 cells were treated with compound **7b** in comparison to colchicine for 48 h. The data obtained clearly indicated that this compound (**7b**) showed G_2/M cell arrest as compared to the untreated control cells. The tested compound **7b** showed 45% and 91% of cell accumulation in G_2/M phase at concentrations of 125 and 500 nM, respectively (**Fig. 7a**).

Annexin-V FITC assay

HCT116 cells were treated with compound 7b for 24 h at 0.5 μM concentration to examine the apoptotic effect. The results suggested that 97.93% cells were live, 0.96% and 1.08% cells were in early and late apoptotsis stage respectively and 0.03% cells were dead in the untreated HCT116 cells (Fig. 7b). However, in the presence of 0.5 μM 7b, 15.23% of cells were found to be live while 39.47 and 45.26 of cells were in the early and late apoptosis stages and 0.04% cells were necrotic as shown in Fig 7b. This experiment suggests that they significantly induce apoptosis in HCT116 cells.

Journal Name

ARTICLE

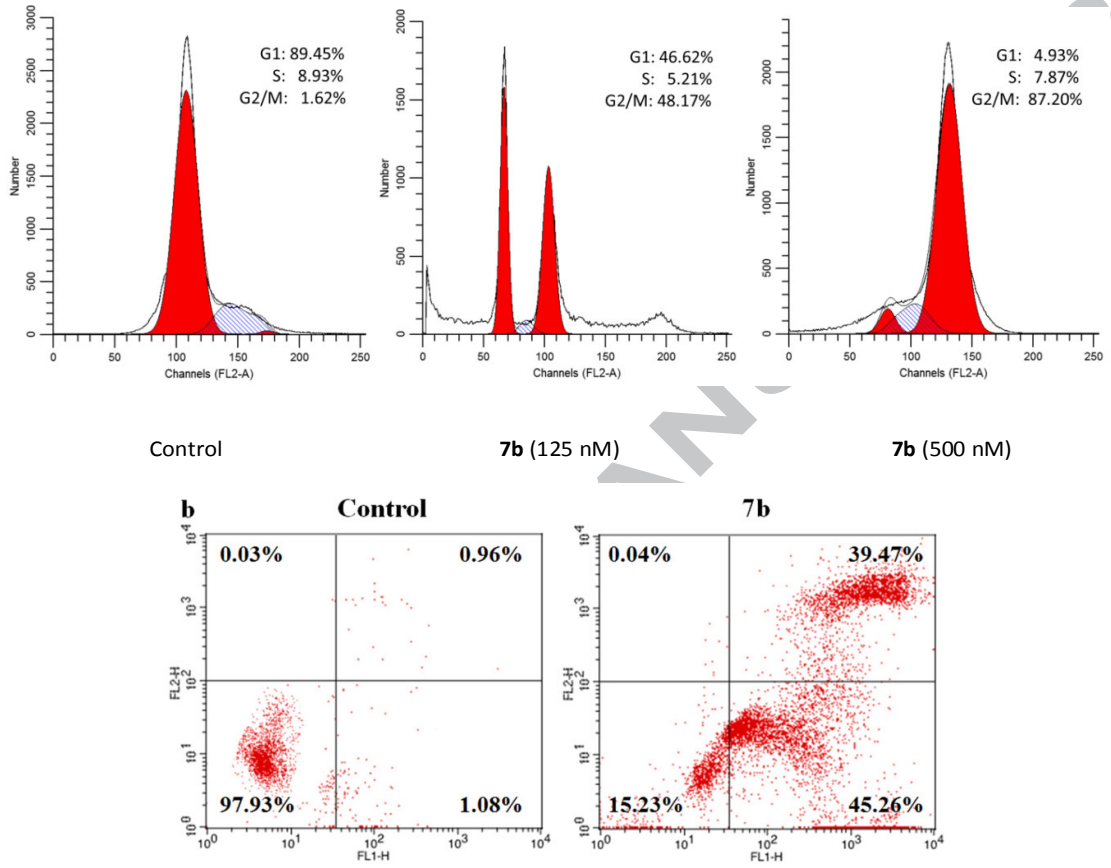

Fig. 7 a). Effects of compound **7b** on HCT116 cell cycle progression. The HCT116 cancer cells were cultured without any compounds (control) or with **7b** at 125 and 500 nM, respectively; **b)**. Flow cytometric analysis of cells stained with annexin V and PI showing the distribution of HCT116 cells in different phases of apoptosis. Cells were incubated with 0.5 µM of **7b** for 24 h.

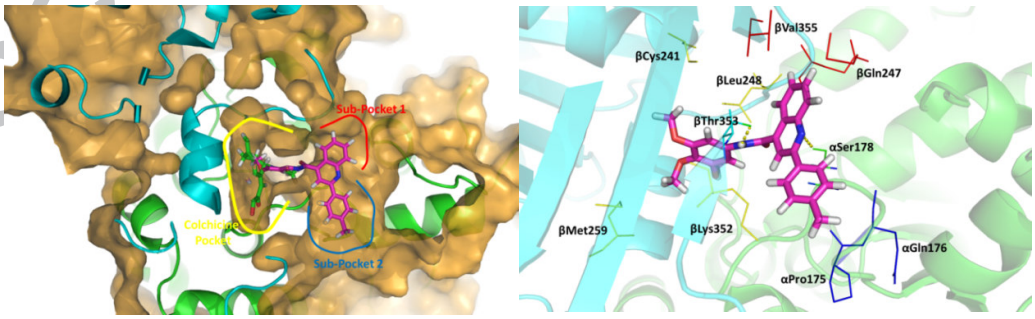

Fig. 8 Predicted binding mode of **7b** with α and β tubulin. a) Overall view of predicted binding model of compound **7b** (magenta, stick model), colchicine (green, stick model) and three binding sub-pockets (red, blue and yellow line) between α (green, ribbon model) and β (light blue, ribbon mode) tubulin. b) Focused view of compound **7b** in the context of surrounding residues (stick model).

Binding model of compound 7b with tubulin

Recently, some progresses were reported to understand the binding mechanism of tubulin domain.[34, 35] To help explore the SARs observed in the in vitro antiproliferation and guide further SAR studies, we proceeded to examine the interaction of compound **7b** with tubulin (PDB code: 4O2B). Molecular docking was performed by simulation of synthetic compounds into the colchicine binding site in tubulin, and the results are shown in **Fig. 8**. All docking runs were applied using the AutoDock 4.2 docking tool.[36] The binding model of compound **7b** and tubulin is depicted in **Fig. 8**. The amino acid residue which had interaction with tubulin is labelled. The results show that compound **7b** partly shares the binding pocket of colchicine, displaying interactions with βCys241, βLys254, βMet259, βIle318, βAsn249, βLys352, αThr179 and αSer178 in the α,β-tubulin, and mostly buried in the β-subunits (**Fig. 8**a). The trimethoxyphenyl group occupies the hydrophobic binding site in the tubulin with βLeu248, βLys352, βMet259 and βCys241. The 4'-methylbenzene moiety occupies the hydrophobic binding site in the tubulin with βLeu333, βAla354, αGln176 and αPro175. The quinoline moiety occupies another small hydrophobic binding site in the tubulin with βMet325, βGln247 and βVal355. In addition, two hydrogen-bonding interactions were observed: one formed by the hydrogen atom of the amide in **7b** and the carboxyl oxygen atom of βThr353 (bond length: C=O…H = 2.1 Å), the other by the nitrogen atom of the quinoline ring and the amino hydrogen atom of αSer178 (bond length: N–H…N = 3.1 Å). The 3D model of the interaction between compound **7b** and the colchicine bonding site is shown in **Fig. 8b**. It was found that the hydrophobic pockets of the colchicine binding site were partly occupied by compound **7b**, and two sub-hydrophobic pockets between α,β-tubulin units were also occupied by compound **7b**. Overall, the binding model suggests that compound **7b** is a potential inhibitor of tubulin.

In addition, some of ADMET properties of 7b were calculated by using Accelry Discovery Studio software V3.5, (supporting information Table S1). The results showed compound 7b possible have good intestinal absorption and aqueous solubility, but needed to improve hepatotoxicity.

Conclusions

In summary, a new class of 2-phenylquinoline-4-carboxamide derivatives was prepared and tested for its anticancer potential against five human cancer cell lines and one human normal cell line. All the compounds exhibited promising antiproliferation activity at micromolar (μM) concentrations. Among the series compounds, **7b** showed significant anticancer activity in human ovarian cancer and human colon cancer with IC_{50} values 0.5 and 0.2 μM, respectively. This compound (**7b**) arrested cell cycle progression in G_2/M phase and inhibited tubulin polymerization. Notably, active compound **7b** exhibited high antiproliferation potency against cancer cell lines (SK-OV-3 and HCT116), but low cytotoxic activity against human normal cell line MRC-5. The current results also revealed additional SAR information. (1) The methoxy moiety on the 4-carboxamide phenyl ring is modifiable to enhance or maintain antitumour activity (**5a**, **6a**, **6c**, **6e**), but a bulky group is unfavourable (**6b**). (2) A para-methyl group on the 2-phenyl ring of quinoline is a better moiety than meta-methyl, ortho-methyl and an electron-withdrawing group (CF_3). (3) No substituted group on the C_7 position of quinoline is favourable due to the steric hindrance between the α,β-tubulin units. Molecular modelling results provided additional insight into the interaction of **7b** with the tubulin colchicine site. These current results will help us to further optimize and develop new drug candidates for clinical studies as novel tubulin inhibitors.

Experimental

Chemistry

All chemicals and reagents used were of commercial grade and were used without any further purification. The reactions were monitored by thin layer chromatography (TLC) using silica gel GF254. Column chromatography was performed with 200–300 mesh silica gel. All yields refer to isolated products after purification. The intermediates and products synthesized were fully characterized by spectroscopic data. The NMR spectra were recorded on a Bruker DRX-500 (^{1}H: 500 MHz, ^{13}C: 125 MHz) using $CDCl_3$ and DMSO-d_6 as solvents. Chemical shifts (δ) are expressed in parts per million (ppm) and J values are given in hertz (Hz). IR spectra were recorded on an FT-IR Thermo Nicolet Avatar 360 using a KBr pellet. HRMS was performed on an Agilent LC/MSD TOF instrument. The melting points were measured by XT-4A melting point apparatus without correction.

General procedure for the preparation of substitutional isatin (3a–d)

Redistilled water (30 mL, 45 °C), sodium sulphate (45 g, 32.0 mmol) and chloral hydrate (4.96 g, 30.0 mmol) were added in turn to a 250 mL three-necked bottle under stirring. A solution of substituted aniline **1a–d** (20.0 mmol) in 35 mL of water containing concentrated hydrochloric acid (5 mL) was then slowly added dropwise into the above mixture. When flocculent precipitate was generated, hydroxylamine hydrochloride (4.52 g, 65.0 mmol) was added to the reaction mixture and stirring was continued for 2 h at 80 °C. A white solid was afforded, and the precipitate was collected by filtration and recrystallization to get the intermediate compounds **2a–d**. Concentrated sulfuric acid was charged into a 150 mL round-bottom flask and slowly warmed to 60 °C followed by addition of intermediates **2a–d** (3.28 g, 20 mmol) in time. After 30 min, the temperature rose to 90 °C and the mixture was stirred at this temperature for 1.5–2 h. The mixture was cooled to room temperature. Then the mixture was poured into water (65 mL) with stirring, hydrolysed for 1 h, and the orange precipitate was collected by filtration to

obtain crude product. The crude product was purified by silica gel column chromatography and eluted with a mixture of EtOAc/petroleum ether (1:5, v/v) to afford **3a–3d** as red solids.

General procedure for the synthesis of 2-phenyl-4-quinoline carboxylic acid (4a–n)

To a 100 mL round-bottom flask, isatin **3a–d** (34.0 mmol), substituted acetophenone (40.8 mmol) and KOH (102 mmol) in ethanol (40 mL) were added with stirring. The resulting mixture was heated to reflux at 85 °C for 3 days. After removing the solvent under reduced pressure, the mixture was dissolved in water and washed twice with ether. The aqueous layer was concentrated and adjusted to pH 2 with concentrated HCl to afford an orange solid. This solid was filtered, washed with water until neutral, dried and purified by flash column chromatography on silica gel and eluted with a mixture of EtOAc/petroleum ether (1:1, v/v) to afford **4a–n** as orange solids.

General procedure for the synthesis of the carboxamide derivatives (5–9)

Method 1: To a 25 mL round-bottom flask, 2-phenyl-4-quinoline carboxylic acid **4a–n** (1.5 mmol) and substituted aniline (1.5 mmol) were added, dissolved in appropriate DMF and followed by the addition of HOBT (1.5 mmol) with stirring. After 15 min, EDCI (1.5 mmol) and TEA (1.5 mmol) were added and the reaction mixture was stirred for 4 h at room temperature. The reaction solution was poured into water and the product was extracted with EtOAc three times. The combined organic phases were washed with HCl (1 N), $NaHCO_3$ (1 N), dried over anhydrous Na_2SO_4 and concentrated under reduced pressure to give crude product. The crude compound was then purified by recrystallization to afford compounds **5–9**.

Method 2: To a 25 mL round-bottom flask, 2-phenyl-4-quinoline carboxylic acid (5.0 mmol) was added, dissolved in appropriate THF and a few drops of DMF were added. Then the mixture was cooled in an ice bath and sulfoxide chloride was slowly dropped into it with stirring for 30 min. The resulting solution was warmed slowly to 45 °C, stirred at this temperature for 6 h and the solvent was evaporated off at low pressure to give a crude residue. Methyl 3-aminothiophene-2-carboxylate (0.31 g, 2.0 mmol) and trimethylamine (0.10 g, 1.0 mmol) were added to a 25 mL round-bottom flask, dissolved in appropriate THF, and the solution of the above crude residue in THF was added dropwise with stirring in an ice bath. The reaction mixture was stirred at room temperature for 4 h. The solvent was evaporated under reduced pressure and the crude product purified by flash column chromatography on silica gel and eluted with a mixture of EtOAc/petroleum ether (1:8, v/v) to afford **5–9**.

Methyl 3-(2-phenylquinoline-4-carboxamido)thiophene-2-carboxylate (5a). Yellow solid; yield: 36.6%; mp 202.0–203.2 °C; IR (KBr): 3432, 2316, 1674, 1576, 1442, 1286 cm^{-1}; ^1H NMR (500 MHz, DMSO-d_6): δ 3.76 (s, 3H, CH_3), 7.38–7.53 (m, 5H, ArH), 7.68–7.71 (t, 1H, ArH), 8.06 (s, 1H, ArH), 8.11–8.13 (d, *J* = 7.5 Hz, 2H, ArH), 8.15–8.17 (d, *J* = 8.45 Hz, 1H, ArH), 8.28–8.29 (d, *J* = 5.4 Hz, 2H, ArH), 10.86 (s, 1H, NH); ^{13}C NMR (125 MHz, DMSO-d_6): δ 16.94, 51.13, 66,63, 87.62, 110.58, 115.82, 121.38, 122.29, 123.93, 126.55, 127.93, 128.73, 129.29, 130.95, 135.66, 137.84, 140.66, 143.11, 148.01, 155.93, 163.59, 163.73; HRMS (TOF ES^+): *m/z* calcd for $C_{22}H_{17}N_2O_3S$ $[M+H]^+$, 389.0954; found, 389.0953.

Methyl-3-(2-phenylquinoline-4-carboxamido)-1,4-dihydropyrazine-2-carboxylate (5b). Brown oil; yield: 33.1%; IR (KBr): 3436, 2981, 1722, 1590, 1242, 1194, 1062, 989, 865, 721cm^{-1}; ^1H NMR (300 MHz, DMSO-d_6): δ 3.82 (s, 3H, CH_3), 6.38–6.42 (m, 2H, ArH), 7.31–7.39 (m, 3H, ArH), 7.75–7.79 (m, 1H, ArH), 7.91–7.95 (m, 1H, ArH), 8.05–8.11 (m, 2H, ArH), 8.24–8.27 (m, 2H, ArH), 8.33 (d, *J* = 3 Hz, 1H, ArH); ^{13}C NMR (75 MHz, DMSO-d_6): δ 54.09, 78.96, 104.54, 111.06, 118.87, 119.79, 122.39, 125.75, 126.74, 128.29, 129.06, 129.17, 129.56, 131.20, 137.36, 142.93, 146.50, 155.44, 165.24, 169.02; HRMS (TOF ES^+): *m/z* calcd for $C_{22}H_{19}N_4O_3$ $[M+H]^+$, 387.1452; found, 387.1454.

N-(5-methylisoxazol-3-yl)-2-phenylquinoline-4-carboxamide (5c). Red solid; yield: 40.9%; mp 206.5–207.8 ℃; IR (KBr): 3207, 1688, 1617, 1549, 1475, 1426, 1275, 761 cm^{-1}; ^1H NMR (500 MHz, DMSO-d_6): δ 1.84 (s, 3H, CH_3), 6.81 (s, 1H, ArH), 7.36–7.45 (m, 4H, ArH), 7.63 (t, *J* = 7.0 Hz, 1H, ArH), 8.06–8.08 (m, 2H, ArH), 8.13 (d, *J* = 8.3 Hz, 2H, ArH), 8.21 (d, *J* = 8.2 Hz, 1H, ArH), 11.46 (s, 1H, NH); ^{13}C NMR (125 MHz, DMSO-d_6): δ 11.97, 96.57, 117.29, 123.31, 124.99, 127.40, 128.76, 129.68, 130.08, 138.63, 140.33, 148.78, 156.46, 158.42, 165.56, 170.36; HRMS (TOF ES^+): *m/z* calcd for $C_{20}H_{16}N_3O_2$ $[M+H]^+$, 330.1237; found, 330.1234.

N-(3-methoxyphenyl)-2-phenylquinoline-4-carboxamide (5d). White solid; yield: 40.2%; mp 191.1–192.1 ℃; IR (KBr): 3419, 1679, 1589, 1446, 1033, 751 cm^{-1}; ^1H NMR (500 MHz, DMSO-d_6): δ 3.74 (s, 3H, CH_3), 6.76 (d, *J* = 7.9 Hz, 1H, ArH), 7.30–7.41 (m, 2H, ArH), 7.54–7.69 (m, 5H, ArH), 7.84 (t, *J* = 7.4 Hz, 1H, ArH), 8.17 (d, *J* = 8.0 Hz , 2H, ArH), 8.35 (t, *J* = 7.5 Hz, 3H, ArH), 10.82 (s, 1H, NH); ^{13}C NMR (500 MHz, DMSO-d_6): δ 55.47, 106.24, 110.04, 112.68, 117.19, 123.57, 125.47, 127.74, 129.30, 130.03, 130.33, 130.69, 138.55, 140.40, 143.40, 148.34, 156.23, 159.97, 165.73; HRMS (TOF ES^+): *m/z* calcd for $C_{23}H_{19}N_2O_2$ $[M+H]^+$, 355.1441; found, 355.1442.

N-(allylcarbamothioyl)-2-phenylquinoline-4-carboxamide (5e). Yellow solid; yield: 71.4%; mp 102.6–103.8 ℃; IR (KBr): 3417, 2922, 2855, 2234, 1709, 1595, 1546, 1453, 1346, 1247, 1199, 1116, 950, 766, 688 cm^{-1}; ^1H NMR (500 MHz, DMSO-d_6): δ 4.36 (s, 2H, CH_2), 5.45–5.60 (m, 2H, $=CH_2$), 6.06 (t, *J* = 6.9 Hz, 1H, $CH=CH_2$), 7.52–7.60 (m, 4H, ArH), 7.65 (t, *J* = 7.5 Hz, 1H, ArH), 7.83 (t, *J* = 7.3 Hz, 1H, ArH), 7.92 (d, *J* = 8.2 Hz, 1H, ArH), 8.07 (s, 1H, NH), 8.20–8.22 (m, 2H, ArH), 8.29 (d, *J* = 8.4 Hz, 1H, ArH); ^{13}C NMR (125 MHz, DMSO-d_6): δ 49.6, 109.32, 117.37, 122.31, 123.75, 127.55, 128.03, 128.57, 128.83, 128.94, 129.93, 130.60, 130.64, 137.33, 138.45, 148.72,

156.54, 166.75; HRMS (TOF ES$^+$): *m/z* calcd for $C_{20}H_{18}N_3OS$ [M–HS]$^+$, 314.1288; found, 314.1286.

N-(4-methoxyphenyl)-2-phenylquinoline-4-carboxamide (6a). Yellow solid; yield: 83.5%; mp 165.3–167.0 ℃; IR (KBr): 3277, 2916, 2873, 1565, 1550, 1499, 1493, 1410, 1349, 1224, 1078, 964 , 827, 702, 639cm^{-1}; ^{1}H NMR (300 MHz, DMSO-d$_6$): δ 3.80 (s, 3H, CH_3), 6.91 (dt, *J* = 7.7 1.0 Hz, 1H), 7.34–7.36 (m, 3H, ArH), 7.58 (d, *J* = 3.0 Hz, 2H, ArH), 7.77–7.85 (m, 2H, ArH), 8.07–8.09 (m, 2H, ArH), 8.15 (d, *J* = 6.0 Hz, 1H, ArH), 8.30–8.32 (m, 1H, ArH), 8.53 (s, 1H, ArH); ^{13}C NMR (75 MHz, DMSO-d$_6$): δ 55.54, 114.30, 118.01, 122.32, 123.44, 124.28, 126.80, 128.29, 129.06, 129.56, 130.37, 131.20, 131.29, 138.41, 147.70, 156.60, 156.64, 167.50; HRMS (TOF ES$^+$): *m/z* calcd for $C_{23}H_{19}N_2O_2$ [M+H]$^+$, 355.1441; found, 255.1445.

N-(4-ethoxyphenyl)-2-phenylquinoline-4-carboxamide (6b). Orange solid; yield: 83.2%; mp 202.5–203.7 ℃; IR (KBr): 3296, 2970, 1644, 1588, 1514, 1397, 1229 cm^{-1}; ^{1}H NMR (500 MHz, DMSO-d$_6$): δ 1.31–1.37 (m, 3H, CH_3), 4.02–4.07 (m, 2H, CH_2), 6.99 (d, *J* = 9.0 Hz, 2H, ArH), 7.54–7.62 (m, 3H, ArH), 7.67–7.70 (m, 2H, ArH), 7.76 (d, *J* = 8.8 Hz, 2H, ArH), 7.85–7.88 (m, 1H, ArH), 8.19 (t, *J* = 9.5 Hz, 2H, ArH), 8.31–8.40 (m, 4H, ArH), 10.73 (s, 1H, NH); ^{13}C NMR (125 MHz, DMSO-d$_6$): δ 15.56, 64.06, 115.37, 117.68, 122.48, 126.08, 128.24, 128.89, 129.80, 130.51, 130.81, 131.15, 132.78, 139.09, 144.08, 148.85, 156.02, 156.74, 165.74; HRMS (TOF ES$^+$): *m/z* calcd for $C_{24}H_{20}N_2O_2Na$ [M+Na]$^+$, 391.1417; found, 391.1419.

2-phenyl-N-(3, 4, 5-trimethoxyphenyl)quinoline-4-carboxamide (6c). Yellow solid; yield: 78.1%; mp 213.4–214.3 ℃; IR (KBr): 3411, 3070, 2956, 2880, 1601, 1532, 1440, 1367, 1271, 1159, 1116, 1051, 826, 766, 716 cm^{-1}; ^{1}H NMR (300 MHz, DMSO-d$_6$): δ 3.88 (s, 9H, OCH_3), 6.58 (s, 2H, ArH), 7.31–7.39 (m, 3H, ArH), 7.75–7.86 (m, 2H, ArH), 8.05–8.10 (m, 2H, ArH), 8.15 (ddd, *J* = 7.7, 1.5, 0.8 Hz, 1H, ArH), 8.30–8.33 (m, 1H, ArH), 8.53 (s, 1H, ArH); ^{13}C NMR (75 MHz, DMSO-d$_6$): δ 56.30, 61.40, 102.69, 118.01, 123.44, 124.28, 126.80, 128.29, 129.06, 129.56, 130.37, 131.20, 133.92, 138.41, 140.64, 147.70, 152.28, 156.64, 167.22; HRMS (TOF ES$^+$): *m/z* calcd for $C_{23}H_{19}N_2OS$ [M+H]$^+$, 371.1213; found, 371.1214.

N-(3-(methylthio)phenyl)-2-phenylquinoline-4-carboxamide (6d). Red solid; yield: 72.6%; mp 189.1–190.3 ℃; IR (KBr): 3233, 3053, 1675, 1588, 1533, 1412, 1348, 1254, 764, 697 cm^{-1}; ^{1}H NMR (500 MHz, DMSO-d$_6$): δ 2.49 (s, 3H, CH_3), 7.02 (s, 1H, ArH), 7.28 (s, 1H, ArH), 7.50 (s, 1H, ArH), 7.55 (s, 2H, ArH), 7.61 (s, 2H, ArH), 7.79 (s, 1H, ArH), 7.83 (s, 1H, ArH), 8.16 (t, *J* = 9.7 Hz, 2H, ArH), 8.25 (d, *J* = 8.0 Hz, 1H, ArH), 8.30 (s, 1H, ArH), 10.71 (s, 1H, NH); ^{13}C NMR (125 MHz, DMSO-d$_6$): δ 15.33, 78.55, 78.82, 79.01, 116.84, 117.12, 117.71, 121.88, 123.58, 125.42, 127.30, 127.54, 128.99, 129.25, 129.96, 130.20, 138.67, 139.13, 139.64, 142.98, 148.49, 156.22, 165.76; HRMS (TOF ES$^+$): *m/z* calcd for $C_{23}H_{19}N_2OS$ [M+H]$^+$, 371.1213; found, 371.1214.

N-(4-methoxy-2-methylphenyl)-2-phenylquinoline-4-carboxamide (6e). Grey solid; yield: 91.2%; mp 207.6–208.9 ℃; IR (KBr): 3793, 3434, 3264, 1645, 1587, 1518, 1412, 1282, 1222, 762 cm^{-1}; ^{1}H NMR (500 MHz, DMSO-d$_6$): δ 2.37 (s, 3H, CH_3), 3.80 (s, 3H, OCH_3), 6.87–6.89 (m, 1H, ArH), 6.93 (s, 1H, ArH), 7.47 (d, *J* = 8.6 Hz, 1H, ArH), 7.55 (t, *J* = 7.2 Hz, 1H, ArH), 7.61 (t, *J* = 7.1 Hz, 2H, ArH), 7.70 (t, *J* = 7.4 Hz, 1H, ArH), 7.86 (t, *J* = 7.5 Hz, 1H, ArH), 8.20 (d, *J* = 8.4 Hz, 1H, ArH), 8.29 (d, *J* = 8.1 Hz, 1H, ArH), 8.39 (d, *J* = 9.4 Hz, 3H, ArH), 10.24 (s, 1H, NH); ^{13}C NMR (125 MHz, DMSO-d$_6$): δ 18.67, 55.59, 111.81, 115.88, 117.26, 123.87, 125.62, 127.74, 128.10, 128.93, 129.31, 130.01, 130.62, 135.45, 138.66, 143.58, 148.37, 156.25, 157.91, 166.06; HRMS (TOF ES$^+$): *m/z* calcd for $C_{24}H_{21}N_2O_2$ [M+H]$^+$, 369.1598; found, 369.1596.

N-(5-chloro-2, 4-dimethoxyphenyl)-2-phenylquinoline-4-carboxamide (6f). Grey solid; yield: 60.9%; mp 251.8–253.6 ℃; IR (KBr): 3386, 1666, 1593, 1523, 1454, 1391, 1201, 1025 cm^{-1}; ^{1}H NMR (500 MHz, DMSO-d$_6$): δ 3.92 (s, 6H, OCH_3), 6.95 (s, 1H, ArH), 7.54 (t, *J* = 7.0 Hz, 1H, ArH), 7.60 (t, *J* = 7.2 Hz, 2H, ArH), 7.68 (t, *J* = 7.5 Hz, 1H, ArH), 7.85 (t, *J* = 7.3 Hz, 1H, ArH), 7.94 (s, 1H, ArH), 8.17 (d, *J* = 8.4 Hz, 1H, ArH), 8.24 (d, *J* = 8.3 Hz, 1H, ArH), 8.31 (s, 1H, ArH), 8.36 (d, *J* = 7.6 Hz, 2H, ArH), 10.14 (s, 1H, NH); ^{13}C NMR (125 MHz, DMSO-d$_6$): δ 56.76, 56.86, 98.55, 111.46, 117.33, 119.88, 123.77, 125.66, 126.31, 127.63, 127.70, 129.29, 129.93, 130.27, 130.58, 138.64, 143.34, 148.26, 152.56, 153.33, 156.13, 166.04; HRMS (TOF ES$^+$): *m/z* calcd for $C_{24}H_{20}N_2O_3Cl$ [M+H]$^+$, 419.1157; found, 419.1154.

N-(4-methoxyphenyl)-2-p-tolylquinoline-4-carboxamide (7a). Yellow solid; yield: 82.1%; mp 232.1–233.5 ℃; IR (KBr): 3256, 1642, 1580, 1520, 1413, 1229, 1025 cm^{-1}; ^{1}H NMR (500 MHz, DMSO-d$_6$): δ 2.40 (s, 3H, CH_3), 3.77 (s, 3H, OCH_3), 6.98–7.00 (m, 2H, ArH), 7.38 (d, *J* = 8.1 Hz, 2H, ArH), 7.63–7.66 (m, 1H, ArH), 7.75 (d, *J* = 9.1 Hz, 2H, ArH), 7.81–7.85 (m, 1H, ArH), 8.14–8.19 (m, 2H, ArH), 8.27 (t, *J* = 8.1 Hz, 3H, ArH), 10.70 (s, 1H, NH); ^{13}C NMR (125 MHz, DMSO-d$_6$): δ 21.30, 55.61, 114.32, 116.92, 121.96, 123.59, 125.55, 127.47, 127.63, 129.91, 130.57, 132.39, 135.81, 140.06, 143.49, 148.33, 156.15, 156.23, 165.29; HRMS (TOF ES$^+$): *m/z* calcd for $C_{24}H_{20}N_2O_2$ [M+Na]$^+$, 391.1417; found, 391.1415.

2-(4-methoxyphenyl)-N-(3, 4, 5-trimethoxyphenyl)quinoline-4-carboxamide(7b). Yellow solid; yield: 79.9%; mp 235.1–235.9 ℃; IR (KBr): 3267, 1649, 1596, 1511, 1452, 1411, 1347, 1234, 1130 cm^{-1}; ^{1}H NMR (500 MHz, DMSO-d$_6$): δ 2.42 (s, 3H, CH_3), 3.69 (s, 3H, OCH_3), 3.82 (s, 6H, OCH_3), 7.28 (s, 2H, ArH), 7.40 (d, *J* = 7.9 Hz, 2H, ArH), 7.66 (t, *J* = 7.0 Hz, 1H, ArH), 7.84–7.87 (m, 1H, ArH), 8.17–8.21 (m, 2H, ArH), 8.29 (t, *J* = 7.6 Hz, 3H, ArH), 10.79 (s, 1H, NH); ^{13}C NMR (125 MHz, DMSO-d$_6$): δ 21.30, 56.18, 60.56, 62.30, 98.21, 116.95, 123.47, 125.50, 127.62, 129.93, 130.61, 134.54, 135.42, 135.78, 140.10, 143.25, 148.34, 153.18, 156.14, 165.57; HRMS (TOF ES$^+$): *m/z* calcd for $C_{26}H_{25}N_2O_4$ [M+H]$^+$, 429.1809; found, 429.1805.

N-(4-methoxy-2-methylphenyl)-2-p-tolylquinoline-4-carboxamide (7c). Purple solid; yield: 90.2%; mp 234.4–236.0 ℃; IR (KBr): 3729, 3433, 3275, 2921, 1648, 1593, 1518, 1416, 1349, 1281, 1224, 1112, 1047, 755 cm^{-1}; ^{1}H NMR (500 MHz, DMSO-d$_6$): δ 2.36

(s, 3H, CH_3), 2.43 (s, 3H, CH_3), 3.80 (s, 3H, OCH_3), 6.86–6.93 (m, 2H, ArH), 7.41 (dd, *J* = 7.9, 8.6 Hz, 2H, ArH), 7.67 (t, *J* = 7.7 Hz, 1H, ArH), 7.84 (t, *J* = 7.5 Hz, 1H, ArH), 8.16 (d, *J* = 8.4 Hz, 1H, ArH), 8.26–8.31 (m, 3H, ArH), 8.35 (s, 1H, ArH), 10.22 (s, 1H, NH); ^{13}C NMR (125 MHz, DMSO-d_6): δ 18.67, 21.31, 55.59, 111.79, 115.86, 117.00, 123.76, 125.59, 127.46, 127.63, 128.11, 128.93, 129.92, 130.55, 135.45, 140.04, 143.50, 148.35, 156.15, 157.89, 166.09; HRMS (TOF ES$^+$): *m/z* calcd for $C_{25}H_{23}N_2O_2$ $[M+H]^+$, 383.1754; found, 397.1754.

N-(4-methoxyphenyl)-2-m-tolylquinoline-4-carboxamide (7d). Red solid; yield: 68.2%; mp 205.0–207.6 ℃; IR (KBr): 3729, 3455, 3318, 2352, 1646, 1593, 1520, 1239, 1102, 1024 cm^{-1}; ^{1}H NMR (500 MHz, DMSO-d_6): δ 2.45 (s, 3H, CH_3), 3.77 (s, 3H, OCH_3), 6.98–7.00 (m, 2H, ArH), 7.34 (d, *J* = 7.4 Hz, 1H, ArH), 7.45 (t, *J* = 7.5 Hz, 1H, ArH), 7.64–7.68 (m, 1H, ArH), 7.75 (d, *J* = 8.9 Hz, 2H, ArH), 7.83–7.86 (m, 1H, ArH), 8.16–8.21 (m, 4H, ArH), 8.32 (s, 1H, ArH), 10.70 (s, 1H, NH); ^{13}C NMR (125 MHz, DMSO-d_6): δ 21.50, 55.62, 114.32, 117.19, 121.97, 123.67, 124.92, 125.55, 127.61, 128.23, 129.19, 129.97, 130.61, 130.96, 132.37, 138.51, 143.53, 148.33, 156.24, 156.31, 165.27; HRMS (TOF ES$^+$): *m/z* calcd for $C_{24}H_{21}N_2O_2$ $[M+H]^+$, 369.1598; found, 369.1599.

2-M-tolyl-N-(3, 4, 5-trimethoxyphenyl)quinoline-4-carboxamide (7e). Yellow solid; yield: 69.4%; mp 234.8–236.4 ℃; IR (KBr): 3793, 3729, 3436, 3266, 2939, 1649, 1598, 1512, 1453, 1409, 1233, 1130, 995 cm^{-1}; ^{1}H NMR (500 MHz, DMSO-d_6): δ 2.45 (s, 3H, CH_3), 3.68 (s, 3H, OCH_3), 3.77 (s, 6H, OCH_3), 7.26 (s, 2H, ArH), 7.35 (d, *J* = 7.5 Hz, 1H, ArH), 7.46 (t, *J* = 7.6 Hz, 1H, ArH), 7.66 (t, *J* = 7.5 Hz, 1H, ArH), 7.84 (t, *J* = 7.4 Hz, 1H, ArH), 8.15–8.21 (m, 4H, ArH), 8.32 (s, 1H, ArH), 10.76 (s, 1H, NH); ^{13}C NMR (125 MHz, DMSO-d_6): δ 21.50, 56.17, 60.56, 98.19, 117.21, 123.54, 124.92, 125.50, 127.68, 128.21, 129.21, 129.99, 130.65, 130.99, 134.48, 135.40, 138.47, 138.54, 143.30, 148.32, 153.17, 156.29, 165.54; HRMS (TOF ES$^+$): *m/z* calcd for $C_{26}H_{25}N_2O_4$ $[M+H]^+$, 429.1809; found, 429.1808.

N-(4-methoxy-2-methylphenyl)-2-m-tolylquinoline-4-carboxamide (7f). White solid; yield: 70.6%; mp 193.5–195.5 ℃; IR (KBr): 3793, 3729, 3437, 3276, 1643, 1593, 1520, 1400, 1220, 1036 cm^{-1}; ^{1}H NMR (500 MHz, DMSO-d_6): δ 2.34 (s, 3H, CH_3), 2.46 (s, 3H, CH_3), 3.78 (s, 3H, OCH_3), 6.84–6.91 (m, 2H, ArH), 7.35–7.49 (m, 3H, ArH), 7.67 (t, *J* = 7.4 Hz, 1H, ArH), 7.83 (t, *J* = 7.7 Hz, 1H, ArH), 8.15–8.21 (m, 3H, ArH), 8.25 (d, *J* = 8.3 Hz, 1H, ArH), 8.34 (s, 1H, ArH), 10.20 (s, 1H, NH); ^{13}C NMR (125 MHz, DMSO-d_6): δ 18.69, 21.54, 55.59, 111.79, 115.86, 117.26, 123.84, 124.96, 125.60, 127.61, 128.11, 128.21, 128.92, 129.21, 129.97, 130.59, 130.96, 135.44, 138.52, 143.55, 148.34, 156.33, 157.88, 166.06; HRMS (TOF ES$^+$): *m/z* calcd for $C_{25}H_{26}N_2O_2$ $[M+H]^+$, 383.1754; found, 383.1750.

N-(4-methoxyphenyl)-2-o-tolylquinoline-4-carboxamide (7g). Red solid; yield: 60.1%; mp 193.0–197.1 ℃; IR (KBr): 3233, 3063, 2313, 1732, 1648, 1594, 1511, 1457, 1301, 1239, 1175, 1032, 824, 769 cm^{-1}; ^{1}H NMR (500 MHz, DMSO-d_6): δ 2.47 (s, 3H, CH_3), 3.76 (s, 3H, OCH_3), 6.96–6.99 (m, 2H, ArH), 7.36–7.42 (m, 3H, ArH), 7.62 (d, *J* = 6.7 Hz, 1H, ArH), 7.69–7.75 (m, 3H, ArH), 7.84–7.87 (m, 1H, ArH), 8.13 (d, *J* = 8.3 Hz, 1H, ArH), 8.22 (d, *J* = 8.2 Hz, 1H, ArH); ^{13}C NMR (125 MHz, DMSO-d_6): δ 20.65, 55.60, 114.31, 120.43, 121.97, 123.09, 125.54, 126.41, 127.81, 129.13, 129.87, 130.32, 130.54, 131.29, 132.31, 136.34, 139.88, 142.84, 147.96, 156.24, 159.52, 165.12; HRMS (TOF ES$^+$): *m/z* calcd for $C_{24}H_{21}N_2O_2$ $[M+H]^+$, 369.1598; found, 369.1596.

N-(4-methoxy-2-methylphenyl)-2-m-tolylquinoline-4-carboxamide (7h). Red solid; yield: 56.4%; mp 130.8–131.8 ℃; IR (KBr): 3793, 3729, 3439, 2351, 1646, 1597, 1504, 1452, 1238, 1110, 1041, 757 cm^{-1}; ^{1}H NMR (500 MHz, DMSO-d_6): δ 2.31 (s, 3H, CH_3), 2.47 (s, 3H, CH_3), 3.77 (s, 3H, OCH_3), 6.83–6.85 (m, 1H, ArH), 6.90 (d, *J* = 2.6 Hz, 1H, ArH), 7.37–7.43 (m, 4H, ArH), 7.63–7.64 (m, 1H, ArH), 7.71 (t, *J* = 7.5 Hz, 1H, ArH), 7.85–7.88 (m, 1H, ArH), 7.91 (s, 1H, ArH), 8.13 (d, *J* = 8.3 Hz, 1H, ArH), 8.29 (d, *J* = 8.3 Hz, 1H, ArH), 10.20 (s, 1H, NH); ^{13}C NMR (125 MHz, DMSO-d_6): δ 18.61, 20.64, 55.57, 111.78, 115.83, 120.55, 123.27, 125.59, 126.42, 127.80, 128.12, 128.83, 129.13, 129.86, 130.29, 130.54, 131.28, 135.47, 136.32, 139.96, 142.88, 147.97, 157.89, 159.52, 165.96; HRMS (TOF ES$^+$): *m/z* calcd for $C_{25}H_{23}N_2O_2$ $[M+H]^+$, 383.1754; found, 383.1756.

N-(4-methoxy-2-methylphenyl)-2-(4-(trifluoromethyl)phenyl)-quinoline-4-carboxamide (7i). Brown solid; yield: 33.6%; mp 239.0–239.8 ℃; IR (KBr): 3381, 3261, 2971, 2315, 1637, 1524, 1416, 1325, 1171, 1103, 1051 cm^{-1}; ^{1}H NMR (500 MHz, DMSO-d_6): δ 2.34 (s, 3H, CH_3), 3.75 (s, 3H, OCH_3), 6.85–6.91 (m, 2H, ArH), 7.45 (d, *J* = 8.6 Hz, 1H, ArH), 7.72 (t, *J* = 7.5 Hz, 1H, ArH), 7.87 (t, *J* = 7.2 Hz, 1H, ArH), 7.96 (d, *J* = 8.0 Hz, 2H, ArH), 8.20 (d, *J* = 8.4 Hz, 1H, ArH), 8.28 (d, *J* = 8.3 Hz, 1H, ArH), 8.45 (s, 1H, ArH), 8.58 (d, *J* = 8.1 Hz, 2H, ArH), 10.23 (s, 1H, NH); ^{13}C NMR (125 MHz, DMSO-d_6): δ 14.44, 18.67, 55.57, 111.79, 115.86, 117.47, 124.16, 125.66, 126.21, 128.04, 128.29, 128.50, 128.84, 130.15, 130.92, 135.40, 142.38, 143.93, 148.28, 154.67, 157.89, 165.84; HRMS (TOF ES$^+$): *m/z* calcd for $C_{25}H_{20}F_3N_2O_2$ $[M+H]^+$, 437.1471; found, 437.1473.

2-(Benzo[d][1,3]dioxol-5-yl)-N-(4-methoxyphenyl)quinoline-4-carboxamide(7j). Yellow solid; yield: 62.1%; mp 263.1–264.5 ℃; IR (KBr): 3265, 1651, 1590, 1506, 1449, 1245, 1243, 1036 cm^{-1}; ^{1}H NMR (500 MHz, DMSO-d_6): δ 3.78 (s, 3H, OCH_3), 6.15 (s, 2H, CH_2), 6.99–7.01 (m, 2H, ArH), 7.11–7.13 (m, 1H, ArH), 7.63 (t, *J* = 7.1 Hz, 1H, ArH), 7.76 (d, *J* = 7.4 Hz, 2H, ArH), 7.81 (t, *J* = 7.0 Hz, 1H, ArH), 7.95–7.97 (m, 2H, ArH), 8.12–8.18 (m, 2H, ArH), 8.29 (s, 1H, ArH), 10.73 (s, 1H, NH); ^{13}C NMR (125 MHz, DMSO-d_6): δ 55.62, 101.93, 107.59, 108.93, 114.30, 116.92, 122.01, 122.36, 123.47, 125.50, 127.34, 129.80, 130.54, 132.37, 132.92, 143.34, 148.20, 148.53, 149.33, 155.61, 156.23, 165.27; HRMS (TOF ES$^+$): *m/z* calcd for $C_{24}H_{18}N_2O_4Na$ $[M+Na]^+$, 421.1159; found,421.1158.

N-(4-methoxyphenyl)-6-methyl-2-p-tolylquinoline-4-carboxamide (8a). Red solid; yield: 81.2%; mp 255.5–255.9 ℃; IR (KBr): 3433, 3278, 1646, 1588, 1518, 1233, 1025, 824 cm^{-1}; ^{1}H NMR (500 MHz, DMSO-d_6): δ 2.39 (s, 3H, CH_3), 2.50 (s, 3H, CH_3), 3.77 (s, 3H, OCH_3), 6.98 (d, *J* = 8.9 Hz, 2H, ArH), 7.36 (d, *J* = 8.0 Hz, 2H, ArH), 7.65 (d, *J* = 8.7 Hz, 1H, ArH), 7.75 (d, *J* = 8.9 Hz, 2H, ArH), 7.94 (s, 1H,

ArH), 8.04 (d, *J* = 8.6 Hz, 1H, ArH), 8.24 (t, *J* = 8.2 Hz, 3H, ArH), 10.68 (s, 1H, NH); ^{13}C NMR (125 MHz, DMSO-d_6): δ 21.28, 21.77, 55.61, 114.30, 116.87, 121.95, 123.54, 124.20, 127.47, 129.69, 129.87, 132,44, 132.68, 135.90, 137.06, 139.80, 142.81, 146.97, 155.21, 156.21, 165.43; HRMS (TOF ES$^+$): *m/z* calcd for $C_{25}H_{22}N_2O_2Na$ $[M+Na]^+$, 405.1573; found, 405.1577.

6-Methyl-2-p-tolyl-N-(3, 4, 5-trimethoxyphenyl)quinoline-4-carboxamide (8b). White solid; yield: 80.1%; mp 236.1–237.6 ℃; IR (KBr): 3432, 3266, 1648, 1593, 1510, 1411, 1234, 1131 cm^{-1}; ^{1}H NMR (500 MHz, DMSO-d_6): δ 2.41 (s, 3H, CH_3), 2.51 (s, 3H, CH_3), 3.69 (s, 3H, OCH_3), 3.79 (s, 6H, OCH_3), 7.28 (s, 2H, ArH), 7.39 (d, *J* = 8.0 Hz, 2H, ArH), 7.68 (d, *J* = 8.6 Hz, 1H, ArH), 7.95 (s, 1H, ArH), 8.05 (d, *J* = 8.6 Hz, 1H, ArH), 8.25 (d, *J* = 8.4 Hz, 3H, ArH), 10.76 (s, 1H, NH); ^{13}C NMR (125 MHz, DMSO-d_6): δ 21.28, 21.75, 56.18, 60.56, 98.20, 116.91, 123.42, 124.11, 127.47, 129.71, 129.89, 132.73, 134.51, 135.47, 135.87, 137.16, 139.84, 142.58, 146.97, 153.17, 155.20, 165.71; HRMS (TOF ES$^+$): *m/z* calcd for $C_{27}H_{26}N_2O_4Na$ $[M+Na]^+$, 465.1785; found, 465.1792.

N-(4-methoxy-2-methylphenyl)-6-methyl-2-p-tolylquinoline-4-carboxamide (8c). White solid; yield: 91.1%; mp 217.1–218.0 ℃; IR (KBr): 3793, 3729, 3433, 3247, 1649, 1594, 1516, 1448, 1286, 1237, 1042, 820 cm^{-1}; ^{1}H NMR (500 MHz, DMSO-d_6): δ 2.36 (s, 3H, CH_3), 2.42 (s, 3H, CH_3), 2.55 (s, 3H, CH_3), 3.80 (s, 3H, OCH_3), 6.87–6.92 (m, 2H, ArH), 7.40 (dd, *J* = 7.8, 8.5 Hz, 3H, ArH), 7.68 (d, *J* = 8.3 Hz, 1H, ArH), 8.04–8.30 (m, 5H, ArH), 10.19 (s, 1H, NH); ^{13}C NMR (125 MHz, DMSO-d_6): δ 18.65, 21.29, 21.83, 55.59, 111.78, 115.86, 116.98, 123.73, 124.32, 127.48, 128.10, 128.98, 129.69, 129.88, 132.64, 135.35, 135.99, 136.98, 139.78, 142.79, 147.01, 155.24, 157.85, 166.20; HRMS (TOF ES$^+$): *m/z* calcd for $C_{26}H_{25}N_2O_2$ $[M+H]^+$, 397.1911; found, 397.1903.

6-Chloro-N-(4-methoxyphenyl)-2-phenylquinoline-4-carboxamide (8d). Yellow solid; yield: 61.6%; mp 275.1–278.9 ℃; IR (KBr): 3290, 1647, 1589, 1520, 1519, 1250, 1120 cm^{-1}; ^{1}H NMR (500 MHz, DMSO-d_6): δ 3.79 (s, 3H, OCH_3), 7.00 (d, *J* = 8.9 Hz, 2H, ArH), 7.55–7.62 (m, 3H, ArH), 7.78 (d, *J* = 8.7 Hz, 2H, ArH), 7.86–7.89 (m, 1H, ArH), 8.19 (d, *J* = 9.0 Hz,1H, ArH), 8.27 (d, *J* = 2.1 Hz, 1H, ArH), 8.38 (d, *J* = 7.3 Hz, 2H, ArH), 8.45 (s, 1H, ArH), 10.88 (s, 1H, NH); ^{13}C NMR (125 MHz, DMSO-d_6): δ 55.63, 114.30, 118.61, 122.20, 124.41, 127.84, 129.32, 130.56, 131.11, 132.14, 132.22, 138.22, 142.08, 146.87, 156.35, 156.78, 164.65; HRMS (TOF ES$^+$): *m/z* calcd for $C_{23}H_{18}N_2O_2Cl$ $[M+H]^+$, 389.1051; found, 389.1053.

6-Chloro-2-phenyl-N-(3, 4, 5-trimethoxyphenyl)quinoline-4-carboxamide (8e). Red solid; yield: 60.8%; mp 256.3–260.1 ℃; IR (KBr): 3440, 2929, 1644, 1546, 1509, 1453, 1415, 1384, 1346, 1233, 1131, 1048, 777 cm^{-1}; ^{1}H NMR (500 MHz, DMSO-d_6): δ 3.69 (s, 3H, OCH_3), 3.81 (s, 6H, OCH_3), 7.25 (s, 2H, ArH), 7.56–7.62 (m, 3H, ArH), 7.86 (d, *J* = 9.0 Hz, 1H, ArH), 8.19 (d, *J* = 9.0 Hz, 1H, ArH), 8.27 (s, 1H, ArH), 8.36 (d, *J* = 7.8 Hz, 2H, ArH), 8.41 (s, 1H, ArH), 10.77 (s, 1H, NH); ^{13}C NMR (125 MHz, DMSO-d_6): δ 56.39, 60.67, 98.70, 118.62, 124.40, 127.90, 129.44, 130.69, 131.28, 132.26, 132.36, 134.94, 135.28, 138.28, 142.11, 147.00, 153.30, 156.89, 166.01; HRMS (TOF ES$^+$): *m/z* calcd for $C_{25}H_{22}N_2O_4Cl$ $[M+H]^+$, 449.1263; found, 449.1259.

6-Chloro-N-(4-methoxy-2-methylphenyl)-2-phenylquinoline-4-carboxamide (8f). Purple solid; yield: 56.9%; mp 232.6–233.1 ℃; IR (KBr): 3395, 2972, 2312, 1640, 1524, 1049 cm^{-1}; ^{1}H NMR (500 MHz, DMSO-d_6): δ 2.35 (s, 3H, CH_3), 3.79 (s, 3H, OCH_3), 6.86 (t, *J* = 6.5 Hz, 1H, ArH), 6.92 (s, 1H, ArH), 7.45 (d, *J* = 8.5 Hz, 1H, ArH), 7.56–7.64 (m, 3H, ArH), 7.88–7.90 (m, 1H, ArH), 8.20 (d, *J* = 8.9 Hz, 1H, ArH), 8.33 (d, *J* = 2.0 Hz, 1H, ArH), 8.38 (d, *J* = 7.3 Hz, 2H, ArH), 8.47 (s, 1H, ArH), 10.31 (s, 1H, ArH); ^{13}C NMR (125 MHz, DMSO-d_6): δ 18.60, 55.60, 111.84, 115.88, 118.57, 124.44, 124.54, 127.82, 128.11, 128.76, 129.35, 130.57, 131.13, 132.15, 135.42, 138.24, 142.10, 146.90, 156.81, 157.96, 165.45; HRMS (TOF ES$^+$): *m/z* calcd for $C_{24}H_{20}N_2O_2Cl$ $[M+H]^+$, 403.1208; found, 403.1212.

6-Fluoro-N-(4-methoxyphenyl)-2-phenylquinoline-4-carboxamide (8g). White solid; yield: 57.5%; mp 207.8–209.6 ℃; IR (KBr): 3434, 3277, 1640, 1519, 1454, 1402, 1242, 1034, 833, 694 cm^{-1}; ^{1}H NMR (500 MHz, DMSO-d_6): δ 3.79 (s, 3H, OCH_3), 7.00 (d, *J* = 8.8 Hz, 2H, ArH), 7.50 (t, *J* = 7.2 Hz, 2H, ArH), 7.56 (t, *J* = 8.5 Hz, 3H, ArH), 7.76 (d, *J* = 8.6 Hz, 2H, ArH), 8.08 (d, *J* = 9.1 Hz, 1H, ArH), 8.30–8.34 (m, 3H, ArH), 10.68 (s, 1H,NH); ^{13}C NMR (125 MHz, DMSO-d_6): δ 14.87, 55.63, 63.96, 104.28, 114.32, 117.67, 122.09, 123.07, 124.88, 127.39, 129.22, 129.83, 131.59, 132.39, 138.74, 141.68, 144.47, 153.64, 156.26, 157.49, 165.45; HRMS (TOF ES$^+$): *m/z* calcd for $C_{23}H_{18}N_2O_2F$ $[M+H]^+$, 373.1347; found, 373.1345.

9-Chloro-N-(4-methoxyphenyl)-5,6-dihydrobenzo[c]acridine-7-carboxamide (9a)

Yellow solid; yield: 40.2%; mp 267.0–269.1 ℃; IR (KBr): 3437, 3241, 1645, 1521, 1116, 624 cm^{-1}; ^{1}H NMR (400 MHz, DMSO-d_6): δ 3.02 (dd, *J* = 4.4 6.4 Hz, 4H, CH_2), 3.77 (s, 3H, OCH_3), 6.98 (d, *J* = 8.8 Hz, 2H, ArH), 7.38–7.48 (m, 3H, ArH), 7.70–7.82 (m, 4H, ArH), 8.15 (d, *J* = 9.2 Hz, 1H, ArH), 8.45–8.48 (m, 1H, ArH), 10.76 (s, 1H, NH); ^{13}C NMR (101 MHz, DMSO-d_6): δ 26.11, 27.28, 55.76, 114.60, 121.88, 123.64, 124.93, 126.16, 127.71, 127.82, 128.72, 130.46, 130.95, 131.95, 133.86, 139.86, 140.67, 145.42, 153.67, 156.52, 164.30; HRMS (TOF ES$^+$): *m/z* calcd for $C_{25}H_{20}ClN_2O_2$ $[M+H]^+$, 415.1208; found, 415.1205.

9-Chloro-N-(4-methoxy-2-methylphenyl)-5,6-dihydrobenzo[c]-acridine-7-carboxamide (9b). Purple solid; yield: 49.9%; mp 272.9–274.5 ℃; IR (KBr): 3790, 3439, 3237, 1645, 1527, 1036, 746 cm^{-1}; ^{1}H NMR (500 MHz, DMSO-d_6): δ 2.33 (s, 2H, CH_2), 2.51 (s, 2H, CH_2), 3.06 (s, 3H, CH_3), 3.79 (s, 3H, OCH_3), 6.92 (s, 2H, ArH), 7.41 (d, *J* = 35.5 Hz, 5H, ArH), 7.86 (s, 3H, ArH), 8.16 (s, 1H, ArH), 8.47 (s, 1H, ArH), 10.23 (s, 1H, NH); ^{13}C NMR (125 MHz, DMSO-d_6): δ 18.68, 26.09, 27.27, 55.64, 60.11, 112.03, 116.03, 123.61, 125.03, 126.08, 127.61, 128.43, 130.28, 130.82, 131.86, 133.83, 134.69, 139.78, 140.86, 145.53, 153.54, 157.87, 165.14; HRMS (TOF ES$^+$): *m/z* calcd for $C_{26}H_{22}ClN_2O_2$ $[M+H]^+$, 429.1364; found, 429.1364.

Biological evaluations

Sulforhodamine B (SRB) assays

Target compounds' inhibition of human cancer cell growth was assessed using the sulforhodamine B assay, as previously described. The panel of cell lines included HCT116 (colon cancer), A549 (lung cancer), and MDA-MB-468 (breast cancer).The growth inhibitory rate of treated cells was calculated by the following formula: [1–(A515treated/A515 control)] × 100%. The results were also expressed as IC_{50} (the compound concentration required for 50% growth inhibition of cancer cells), which was calculated by the Logit method. The mean IC_{50} was determined from the results of three independent tests.

Immunofluorenscence staining

A549 cells (1 × 104) were seeded in 96-well culture plate and incubated for 12 h at 37 ℃ and 5% CO_2. Cells were treatment with DMSO, colchicine, and **7b** for 24 h. The cells were fixed with methanol and then permeabilized with 0.5% Triton X-100/PBS. The cells were incubated overnight with primary antibody (α-tubulin) at 4 °C. After washing three times with PBS, cells were incubated with corresponding fluorescence-conjugated secondary antibody for 1 h. The nuclei of cells were labeled with DAPI. Cells were visualized using a fluorescence microscopy.

In vitro tubulin polymerization

A fluorescence based tubulin polymerization assay was performed accoding to the manufacturers protocol (BK011, Cytoskeleton, Inc.). Briefly, the reaction mixture was taken within a total volume of 10 µL contained PEM buffer, GTP (1 µM) in the presence or absence of the test compound **7b** at a final concentration. In vitro tubulin polymerization was followed by a time dependent increase in fluorescence due to the incorporation of a fluorescene reporter intomicrotubules as polymerization proceeds. Fluorescence emission at 420 nm (excitation wavelength is 360 nm) was measured by using a Biotec multimode plate reader. Polymerization was finally monitored by increase in the fluorescence mentioned above at 37 °C. The IC_{50} value was defined as the drug concentration required for inhibiting 50% of tubulin assembly compared to the control.

Colchicine competition assay

Compound **7b** with different concentration (0.1, 0.5, 1, 5 and 10 µM) was incubated with 3 µM tubulin in the presence and absence of 3µM colchicine in 30µM Tris buffer for 1hr at 37 ℃. CA-4 was used as a positive control, whereas Vinblastine was used as a negative control. After incubation, the fluorescence of the tubulin-colchicine complex was determined by using a Tecan multimode reader at an exitation wavelength of 350 nm and an emission wavelength of 435 nm. Tris buffer (30 mM) was used as blank, which was subtracted from all the samples, and the fluorescence values were normalized to DMSO (control).

Western blot analysis of soluble versus polymerized tubulin

Cells were seeded in 12-well plates at 1 × 10^5 cells per well in complete growth medium. Following treatment of cells with respective compound 7b for a duration of 24 h, cells were washed with PBS and subsequently soluble and insoluble tubulin fractions were collected. To collect the soluble tubulin fractions, cells were permeabilized with 200 µL of pre-warmed lysis buffer [80 mM Pipes-KOH (pH 6.8), 1 mM $MgCl_2$, 1 mM EGTA, 0.2% Triton X-100, 10% glycerol, 0.1% protease inhibitor cocktail (Sigma-Aldrich)] and mixed with 100 µL of 3 × Laemmli's sample buffer (180 mM Tris-Cl pH 6.8, 6% SDS, 15 glycerol, 7.5% β-mercaptoethanol and 0.01% bromophenol blue). Samples were immediately heated to 95 ℃ for 3 min. To collect the insoluble tubulin fraction, 300 µL of 1 × Laemmli's samples buffer was added to the remaining cells in each cell, and the samples were heated to 95 ℃ for 3 min. Equal volumes of samples were run on an SDS-10% polyacrylamide gel and were transferred to a nitrocellulose membrane employing semidry transfer at 50 mA for 1 h. Blots were probed with mouse anti-human α-tubulin diluted 1:2000 ml (Sigma) and stained with rabbit anti-mouse secondary antibody coupled with horseradish peroxidase, diluted 1:5000 ml (Sigma). Bands were visualized using an enhanced Chemiluminescence protocol (Pierce) and radiographic film (Kodak).

Flow cytometric evaluation of apoptosis

HCT116 were seeded in six-well plates and allowed to grow overnight. The medium was then replaced with complete medium containing 0.5 µM concentration of compound 7b for 24 h along with vehicle alone (0.001% DMSO) as the control. After 24 h of drug treatment, the cells from the supernatant and adherent monolayer cells were harvested by trypsinization, and washed with PBS at 3000 rpm. Then the cells were stained with Annexin V-FITC and propidium iodide using the Annexin-V-PI apoptosis detection kit (Sigma Aldrich). Flow cytometry was performed using a FACScan (Becton Dickinson) equipped with a single 488 nm argon laser as described earlier. Annexin V-FITC was analysed using excitation and emission settings of 488 nm and 535 nm (FL-1 channel); PI, 488 nm and 610 (Fl-2 channel).

Molecular modeling

To investigate the binding mode of compound to the tubulin, the advanced docking program Autodock 4.2 tool was used to automatically dock the inhibitor to the enzyme. The crystal structure of tubulin in a complex with its inhibitor colchicine (PDB entry code 4O2B) was recovered from Brookhaven Protein Database (PDB). The missing atoms and residues were modeled in Sybyl 6.8.17. Atomic charges were taken as Kollman-united-atom26 for the macromolecule and Gasteiger–Marsili27 for the inhibitor. To explore the binding mode of compounds to the colchicine binding domain of tubulin, the advanced docking program Autodock 4.2 tool was used to automatically dock the inhibitor to the protein. The Lamarckian genetic algorithm (LGA) was applied to analyze inhibitor–protein interactions. A Solis and Wets local search

performed the energy minimization on a user-specified proportion of the population. The docked conformations of the inhibitor were generated after a reasonable number of evaluations. The whole docking operation in this study can be summarized follows. First, the colchicine binding domain of tubulin was checked for polar hydrogens and assigned for partial atomic charges, then a PDBQ file was created, and the atomic solvation parameters were assigned for the macromolecule. Meanwhile, some of the torsion angles of the inhibitor that would be explored during molecular docking stage were defined, allowing the conformation search for the ligand during the docking process. Second, the grid map with 60 × 60 × 60 points and a spacing of 0.375 Å was calculated using the AutoGrid program in order to evaluate the binding energies between the inhibitor and the macromolecule. Third, some important parameters for LGA calculations were reasonably set (see Box 1), not only the atom types, but also the generations and the number of runs for the LGA algorithm were edited and properly assigned according to the requirements of the Amber force field. The maximum number of generations, energy evaluations and docking runs were set to 3.0 × 105, 1.5 × 107, and 30, respectively. Finally, the docked complex of the inhibitor-enzyme for the inhibitor was selected according to the criterion of interaction energy combined with geometrical matching quality.

Docking simulations were performed using the Lamarckian genetic algorithm (LGA) and the Solis and Wets local search method. Each run of the docking operation was terminated after a maximum of 2500000 energy evaluations.

Acknowledgements

The authors gratefully acknowledge the Program for Changjiang Scholars and Innovative Rsearch Team in University (IRT17R94), the NSFC (Nos. 21662044, 21262043, 81760621 and U1202221), the Foundation of "Yunling Scholar" Program of Yunnan Province for financial support, and thank the High Performance Computing Center at Yunnan University for use of the high performance computing platform.

Notes

The authors declare no competing financial interest.

References

1. K. J. Verhey and J. Gaertig, *Cell Cycle*, **2007**, *6*, 2152–2160.
2. M. A. Jordan and L. Wilson, *Nat. Rev. Cancer*, **2004**, *4*, 253–265.
3. O. Valiron, N. Caudron and D. Job, *Cell. Mol. Life Sci.*, **2001**, *58*, 2069–2084.
4. E. Nogales, Annu. Rev. Bioph. Biom., **2001**, *30*, 397–420.
5. K. H. Downing, Annu. *Rev. Cell Dev. Bi.*, **2000**, *16*, 89–111.
6. V. Verones, N. Flouquet, M. Lecoeur, A. Lemoine, A. Farce, B. Baldeyrou, C. Mahieu, N. Wattez, A. Lansiaux, J. Goossens, P. Berthelot and N. Lebegue, *Eur. J. Med. Chem.*, **2013**, *59*, 39–47.
7. K. Odlo, J. Hentzen, J. F. Dit Chabert, S. Ducki, O. A. B. S. Gani, I. Sylte, M. Skrede, V. A. Florenes and T. V. Hansen, *Bioorg. Med. Chem.*, **2008**, *16*, 4829–4838.
8. E. Pasquier, N. Andre and D. Braguerl, *Curr. Cancer Drug Tar.*, **2007**, *7*, 566–581.
9. A. Jordan, J. A. Hadfield, N. J. Lawrence and A. T. McGown, *Med. Res. Rev.*, **1998**, *18*, 259–296.
10. C. Dumontet and M. A. Jordan, Nat. Rev. Drug Discov., **2010**, *9*, 790–803.
11. Y. Li, J. Liu, N. Liu, D. Shi, X. Zhou, J. Lv, J. Zhu, C. Zheng and Y. Zhou, *Bioorg. Med. Chem.*, **2011**, *19*, 3579–3584.
12. M. M. Cooney, T. Radivoyevitch, A. Dowlati, B. Overmoyer, N. Levitan, K. Robertson, S. L. Levine, K. DeCaro, C. Buchter, A. Taylor, B. S. Stambler and S. C. Remick, Clin. *Cancer Res.*, **2004**, *10*, 96–100.
13. L. V. Beerepoot, S. A. Radema, E. O. Witteveen, T. Thomas, C. Wheeler, S. Kempin and E. E. Voest, *J. Clin. Oncol.*, **2006**, *24*, 1491–1498.
14. A. L. Risinger, C. D. Westbrook, A. Encinas, M. Muelbaier, C. M. Schultes, S. Wawro, J. D. Lewis, B. Janssen, F. J. Giles and S. L. Mooberry, *J. Pharmacol. Exp. Ther.*, **2011**, *336*, 652–660.
15. B. L. Flynn, G. S. Gill, D. W. Grobelny, J. H. Chaplin, D. Paul, A. F. Leske, T. C. Lavranos, D. K. Chalmers, S. A. Charman, E. Kostewicz, D. M. Shackleford, J. Morizzi, E. Hamel, M. K. Jung and G. Kremmidiotis, *J. Med. Chem.*, **2011**, *54*, 6014–6027.
16. T. Owa, A. Yokoi, K. Yamazaki, K. Yoshimatsu, T. Yamori and T. Nagasu, *J. Med. Chem.*, **2002**, *45*, 4913–4922.
17. T. Ashizawa, H. Miyata, H. Ishii, C. Oshita, K. Matsuno, Y. Masuda, T. Furuya, T. Okawara, M. Otsuka, N. Ogo, A. Asai and Y. Akiyama, *Int. J. Oncol.*, **2011**, *38*, 1245–1252.
18. K. Matsuno, Y. Masuda, Y. Uehara, H. Sato, A. Muroya, O. Takahashi, T. Yokotagawa, T. Furuya, T. Okawara, M. Otsuka, N. Ogo, T. Ashizawa, C. Oshita, S. Tai, H. Ishii, Y. Akiyama and A. Asai, *ACS Med. Chem. Lett.*, **2010**, *1*, 371–375.
19. J. Li, J. Chen, C. S. Gui, L. Zhang, Y. Qin, Q. Xu, J. Zhang, H. Liu, X. Shen and H. L. Jiang, *Bioorg. Med. Chem.*, **2006**, *14*, 2209–2224.
20. A. V. Zimichev, M. N. Zemtsova, A. G. Kashaev and Y. N. Klimochkin, *Pharm. Chem. J*, **2011**, *45*, 217–219.
21. K. Metwally, A. Khalil, A. Sallam, H. Pratsinis, D. Kletsas and K. El Sayed, *Med. Chem. Res.*, **2013**, *22*, 4481–4491.
22. K. Metwally, H. Pratsinis and D. Kletsas, *Med. Chem. Res.*, **2015**, *24*, 2604–2611.
23. K. Metwally, H. Pratsinis and D. Kletsas, *Planta Med.*, **2008**, *74*, 1147.
24. K. Metwally, H. Pratsinis and D. Kletsas, *Eur. J. Med. Chem.*, **2007**, *42*, 344–350.
25. J. M. Andreu, B. Perez-Ramirez, M. J. Gorbunoff, D. Ayala and S. N. Timasheff, *Biochemistry-Us*, **1998**, *37*, 8356–8368.

26. B. Perez-Ramirez, M. J. Gorbunoff and S. N. Timasheff, *Biochemistry-Us*, **1998**, *37*, 1646–1661.
27. R. Islam, M. I. Hossain, Y. Okamoto, T. Nagamatsu, K. Anraku and T. Okawara, *Heterocycles*, **2014**, *89*, 693–708.
28. C. A. Herdman, L. Devkota, C. Lin, H. Niu, T. E. Strecker, R. Lopez, L. Liu, C. S. George, R. P. Tanpure, E. Hamel, D. J. Chaplin, R. P. Mason, M. L. Trawick and K. G. Pinney, *Bioorg. Med. Chem.*, **2015**, *23*, 7497–7520.
29. Y. Yin, F. Qiao, L. Jiang, S. Wang, S. Sha, X. Wu, P. Lv and H. Zhu, *Bioorg. Med. Chem.*, **2014**, *22*, 4285–4292.
30. S. Wang, X. Wang, B. Qin, E. Ohkoshi, K. Hsieh, E. Hamel, M. Cui, D. Zhu, M. Goto, S. L. Morris-Natschke, K. Lee and L. Xie, *Bioorg. Med. Chem.*, **2015**, *23*, 5740–5747.
31. M. Yang, Y. Qin, C. Chen, Y. Zhang, B. Li, T. Liu, H. Gong, B. Wang and H. Zhu, *RSC Adv.*, **2016**, *6*, 30412–30424.
32. R. Mahesh, V. L. Nayak, K. S. Babu, S. Riyaz, T. B. Shaik, G. B. Kumar, P. L. Mallipeddi, C. R. Reddy, K. C. Shekar, J. Jose, N. Nagesh and A. Kamal, *ChemMedChem*, **2017**, *12*, 678–700.
33. C. Kanthou, O. Greco, A. Stratford, I. Cook, R. Knight and O. Benzakour, Am. J. Pathol., **2004**, *165*, 1401–1411.
34. M. Athar, M. Yousuf Lone, M. K. V, A. Radadiya, A. Shah and C. J. P, *Comb. Chem.* High Throughput Screen, **2017**.
35. P. Ranjan, S. P. Kumar, V. Kari and P. C. Jha, *Comput. Biol. Chem.*, **2017**, *68*, 78–91.
36. G. M. Morris, R. Huey, W. Lindstrom, M. F. Sanner, R. K. Belew, D. S. Goodsell and A. J. Olson, *J. Comput. Chem.*, **2009**, *30*, 2785–2791.

Abstract

Design, synthesis and biological evaluation of 2-phenylquinoline-4-carboxamide derivatives as a new class of tubulin polymerization inhibitors

Kaixiu Luo[a‡], Li Zhu[a‡], Ke Li[b‡], Yi Jin*[a] and Jun Lin*[a]